RESPONSE TO REFEREE #1

A Fast and Physically Grounded Ocean Model for GCMs: The Dynamical Slab Ocean Model of the Generic-PCM (rev. 3423)

We sincerely thank Referee #1 for their detailed report and constructive criticism, which has been very useful for improving our manuscript. Below, we first provide a response to the general comments and then a point-by-point response. Where appropriate, we indicate how the manuscript will be revised in the final version. We paste the original comments in red and our response in black. Our proposed changes to the manuscript are presented cursive and as separate blocks.

Referee Report (received on 27 Oct 2025)

General Comments

This study presents a computationally efficient ocean model for use in planetary climate simulations, with proposed relevance to the exoplanet modeling community. The manuscript presents a two-layer slab ocean model integrated into the Generic Planetary Climate Model (Generic-PCM). The model aims to balance physical realism with computational speed, making it suitable for long-term simulations and parameter sweeps that are often of interest in the context of exoplanet studies. The work appears to be mainly a follow-up on Codron (2012) and Charnay et al. (2013), who laid important groundwork in representing ocean heat transport in slab models. The dynamical slab ocean model of the Generic-PCM presented here builds on that legacy by improving sea ice representation and including a Gent-McWilliams parameterisation. The model is validated against both an idealized aquaplanet and an Earth scenario, as already done in Codron (2012) and Charnay et al. (2013), with a somewhat more detailed comparison with these two benchmark cases.

Overall, this is an interesting study that can propose an improved modelisation of ocean heat transport mechanisms for applications where computational efficiency and flexibility are paramount. There are several areas that require improvement before publication. These include primarily a more direct comparisons with Codron (2012) and Charnay et al. (2013), with clearer comments regarding the improvements of this new version of the dynamical slab ocean model with respect to previous 2-layer ocean models, and further discussion about the model validation against other scenarios with respect to the ones already considered in previous works. A more detailed analysis of the model validation is presented here compared to Codron (2012) and Charnay et al. (2013), with specific evaluations of seasonal climate and sea ice, which were previously only superficially addressed. However, further validation would have constituted a significant advancement, and an opportunity to test the model capabilities against AOGCM results in different scenarios. Examples include a “ridgeworld” continental configuration, that significantly impacts ocean dynamics, or

non-solar host star spectra, given the newly implemented spectrally dependent parameterisation of sea ice and snow albedo. I therefore recommend a major revision.

We thank the referee for the careful and constructive evaluation. We have substantially revised the manuscript to address the points raised.

In response to the referee's request, we have incorporated more systematic comparisons with Codron (2012) and Charnay et al. (2013) throughout the manuscript. These revisions include: (i) direct overlays of temperature, precipitation and meridional ocean heat transport (OHT) components, (ii) dedicated discussion and appendix sections comparing SST structures and OHT decomposition, and (iii) clearer identification of the physical origin of differences, including the roles of the Sverdrup balance, Gent–McWilliams (GM) transport, and updates to the atmospheric model. Addressing these points required additional simulations, which have ultimately strengthened and clarified the manuscript.

We now emphasise more clearly that the present dynamical slab ocean model improves upon earlier implementations through: (i) inclusion of the Sverdrup balance, (ii) explicit GM eddy parameterisation, (iii) spectrally dependent snow / sea ice albedo, (iv) improved seasonal sea ice representation, and (v) full parallelisation, enabling efficient long integrations and parameter sweeps, particularly important for exoplanet studies.

We appreciate the suggestion to explore additional validation scenarios such as (i) a ridgeworld configuration or (ii) non-solar host star spectra. Regarding (i), ridgeworld configurations primarily induce geostrophic gyre circulations, which relies on horizontal pressure gradients that are not explicitly represented in the present slab ocean model. While investigating the role of continents in ocean dynamics is indeed important, the objective of this manuscript is to introduce and validate the dynamical slab ocean model itself. Therefore, we consider the ridgeworld scenario to be beyond the scope of this development-focused study.

For (ii), we agree that testing the model under non-solar spectral conditions is important, particularly given the new spectrally dependent albedo formulation. A consistent test case would involve a tidally locked planet orbiting an M-dwarf star, which introduces additional dynamical regimes (e.g., slow rotation, altered atmospheric circulation), expanding the scope of this manuscript. Instead, to illustrate the impact of the spectral albedo scheme, we include in this response document a surface albedo map comparing a converged Earth-like simulation under solar irradiation with one under a TRAPPIST-1-like spectrum (the latter integrated for one model year). This shows the expected 40–50% reduction in snow/ice albedo under a 2550 K blackbody-like stellar emission. A full investigation of M-dwarf climates using this framework is the subject of ongoing work.

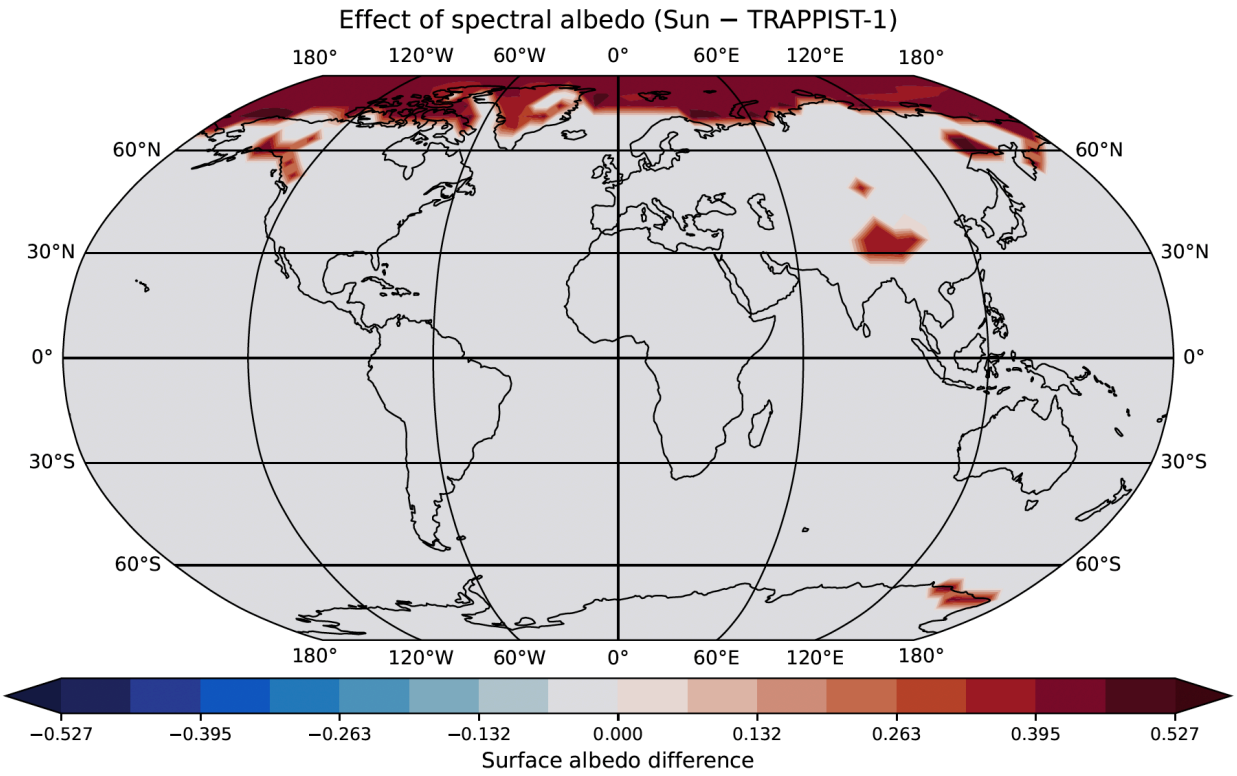

We would like to emphasise that the primary objectives of this manuscript are to: (i) document the improved dynamical slab ocean model, (ii) demonstrate its improvements relative to previous two-layer models and (iii) validate it against aquaplanet and modern Earth configurations. The overarching aim is to provide the community a computationally efficient and flexible tool suitable for exoplanet and paleoclimate studies.

We thank the referee again for the constructive criticism. With the revisions detailed in the responses below, we believe that our manuscript has been significantly strengthened.

Specific Comments

1. Ln 33: In listing applications of dynamic oceans for planetary climate studies, it would be more complete to also include works about Mars (e.g. Schmidt et al. 2022), in addition to Venus.

Thank you for the suggestion, including Mars improves the completeness of the list. We revise the text to read:

"... ancient climates on Earth (e.g., Olson et al., 2022; Ragon et al., 2024), ~~as well as early~~ Venus (e.g., Way et al. 2016; Way and Del Genio, 2020) ***and Mars (e.g., Schmidt et al. 2022)****, where they play …"*

2. Ln 37: Distinguishing between tidal locking and synchronous rotation would be more accurate. As mentioned later in the manuscript, at Ln 566, "tidally locked in a 1:1

spin-orbit resonance" refers to a synchronous rotation case, while "tidally locked" could refer to higher order spin-orbit resonances. In general, this terminology is often improperly used by the community, with "synchronously rotating" and "tidally locked" being adopted interchangeably. However, it would be more consistent and clearer to choose one descriptor within the text.

Thank you for pointing out this relevant specificity. We revise the text in the following places:

*Ln 37: "... and are expected to be in synchronous rotation (tidally locked **in a 1:1 spin-orbit resonance**), having a permanent dayside and nightside …"*

*Ln 44: "Checlair et al. (2019) showed that due to OHT, habitable ~~tidally locked~~ **synchronously rotating** planets are unlikely to have snowball states."*

*Ln 48: "... can shift the thermal hotspot eastward in phase curves of temperate ~~tidally locked~~ **synchronously rotating** planets."*

*Ln 566: "... expected to be **in synchronous rotation** ~~tidally locked in a 1:1 spin-orbit resonance~~, particularly those orbiting …"*

*Ln 610: "These processes may be even more important on ~~tidally locked~~ **synchronously rotating** planets, where strong day–night contrasts …"*

We also take this opportunity to make a subtle change to the following line:

Ln 571: "However, the reduced Coriolis parameter f on slowly rotating ~~tidally locked~~ planets will lead to a larger Rossby …"

3. Ln 38: The spin state of Proxima-b is still debated, with several studies suggesting a 3:2 spin-orbit resonance capture even for small orbital eccentricities (e.g. Ribas et al. 2016).

The text has been revised accordingly to reflect this uncertainty and a footnote added. We also add some seminal papers on spin-orbit resonances and climate to establish more context:

*Ln 36-38: "Most known habitable zone (HZ; Kasting et al., 1993) exoplanets orbit low-mass stars and are expected to **undergo tidal spin-down, often settling into a synchronously rotating** (tidally locked **in a 1:1 spin-orbit resonance; for e.g., see Goldreich & Peale 1966; Pierrehumbert & Hammond 2019),** having a permanent dayside and nightside (Ribas et al., 2016; Turbet et al., 2016, 2018, 2020a**; Braam et al. 2025**) like Proxima-b* (Anglada-Escudé et al., 2016) and TRAPPIST-1e (Gillon et al., 2017) …"*

****However, the spin state of Proxima-b remains uncertain with studies suggesting a 3:2 spin-orbit resonance capture even for modest orbital eccentricities (e.g., Goldreich & Peale 1966; Dobrovolskis 2007; Ribas et al., 2016; Pierrehumbert & Hammond 2019; Valente & Correia 2022)."***

4. Ln 73-79: This work appears to be a follow-up of Codron (2012) and Charnay et al (2013). This should be made clearer in the introduction when these works are

mentioned. While the manuscript presents a well-implemented and computationally efficient “dynamical slab ocean model”, its core architecture and conceptual framework appear to be largely derivative of Codron (2012). Improvements to this model are presented later in the manuscript (in “Model description”), but these enhancements build upon an existing foundation rather than represent a fundamentally new modeling paradigm. I recommend the authors clarify the degree of novelty in the introduction, as the current framing may give the impression that the model is entirely new (Ln 73, as well as in the abstract). The model is more accurately described as a refined and extended implementation of a previously published concept: improvements to the previous model are specified in Ln 77-79, while Ln 74-76 seem to be describing previous work.

We thank the referee for this helpful clarification. Ln 123-127 had previously explicitly mentioned the new additions to the model compared to Codron (2012) and Charnay et al. (2013), but we agree that this should be mentioned in the Introduction instead. Accordingly, we have revised the corresponding paragraphs in the Introduction and omitted Ln 123-127 to avoid repetition:

Ln 73-85: “This paper presents a ***follow-up of the model originally introduced by Codron (2012) and later adapted by Charnay et al. (2013). These earlier models included horizontal diffusion and convection, with Codron (2012) introducing, for the first time in a slab ocean model, wind-driven Ekman transport – the dominant driver of tropical meridional OHT in Earth observations (Levitus, 1987; Forget and Ferreira, 2019). Building upon this foundation, our work refines the two core processes historically handled by the dynamical slab ocean:***

(a) Sea ice evolution; with a spectral albedo representation, refined treatment of ice formation and melting, and the introduction of a finite heat capacity for snow (Section 2.2)

(b) Heat transport by ocean circulation; through optimised horizontal diffusion and Ekman transport, a Sverdrup balance scheme near the equator for more consistent tropical meridional transport (Section 2.3.1), and the implementation of mesoscale eddy mixing via the Gent-McWilliams parameterisation (Gent & McWilliams, 1990; Section 2.3.2), marking its first application within a slab ocean model.

The model is fully parallelised, enabling substantially faster integrations than earlier implementations and making it well suited for long simulations and ensemble studies, important in exoplanet and paleoclimate science. With these developments, our dynamical slab ocean model acts as a bridge between higher-level slab-oceans and fully coupled AOGCMs. ~~*new "dynamical slab ocean model" that bridges the gap between higher-level slab oceans and fully coupled AOGCMs. In our model, OHT is an emergent process that effectively couples the atmosphere and ocean. It includes wind-driven Ekman transport – the dominant driver of tropical meridional OHT in Earth observations \citep{levitus1987meridional,forget2019global} – along with horizontal*~~

~~*diffusion and convection, following \citet{codron2012ekman} and \citet{charnay2013exploring}. Our model also introduces mesoscale eddy mixing in slab oceans through the Gent-McWilliams parameterisation \citep{gent1990isopycnal}, enabling horizontal and vertical temperature mixing. Additionally, sea ice evolution depends on ice thickness and the incoming spectra.*~~

~~*The model is designed to support large ensemble studies — a critical need in exoplanet and paleoclimate science, where observational constraints are sparse, motivating the exploration of a wide parameter space. Our goal is not to match the full complexity of AOGCMs, but to provide the modelling community a faster, physically grounded alternative - an improved compromise over traditional slab ocean models. This philosophy also aligns with the broader philosophy of intermediate-complexity GCMs like \textit{ExoPlaSim} \citep{paradise2022exoplasim}, which enable large-scale explorations of planetary climates while retaining core physical realism.*~~"

Ln 123-127: ~~*In this study, we improve the two key processes historically handled by the dynamical slab ocean: (a)*~~ ~~***Sea ice evolution***~~*, by improving the spectral albedo representation, refining sea ice formation, melting and freezing, and introducing a finite heat 125 capacity for snow (Sect. 2.2); and (b)*~~ ~~***Heat transport by ocean circulation***~~*, by optimising horizontal diffusion and Ekman transport, and implementing a new Gent–McWilliams (advection) parameterisation that captures both, the effect of mesoscale eddies and convection (Sect. 2.3). Furthermore, the model is now fully parallelised, enabling fast computation.*~~

We also modify the abstract for consistency:

Ln 1: "We present ~~*the new*~~ ***an improved*** *dynamical slab ocean model implemented in a 3-D General Circulation Model (GCM) called the Generic Planetary Climate Model (Generic-PCM; formerly the LMD-Generic GCM).* ***Earlier two-layer slab ocean models featured wind-driven Ekman transport, horizontal diffusion and convective adjustment.*** ~~*Our two-layer slab ocean model features emergent ocean heat transport (OHT) arising from wind-driven Ekman transport, horizontal diffusion, convective adjustment, and a newly implemented Gent–McWilliams (GM) parameterisation for mesoscale eddies. Sea ice evolution is spectrally-dependent and varies with ice thickness.*~~ ***Building upon this, our updated parallelised model introduces a Sverdrup balance scheme for Ekman transport, the first application of the Gent–McWilliams (GM) parameterisation of mesoscale eddies in a slab ocean model, and a spectrally dependent, thickness-dependent formulation of sea ice and snow albedo.***"

5. Ln 176: More context for the chosen value of A_ice,max would be helpful. Specifically, the choice of A_ice,max for the VIS needs further explanation. The chosen value is 0.65, consistent to the spectrally-independent value chosen by Charnay et al. (2013), and inconsistent to the higher value of 0.75 chosen by Pedersen et al. (2009) - that was referenced here.

We would like to clarify that our choice of A_ice,max was informed by calibrating our thickness-dependent albedo formulation to the Antarctic sea ice observations of Brandt et al. (2005). The study's Table 3 shows that the VIS albedo of snow-free first-year sea ice typically ranges from 0.54 for thinner ice up to 0.67 for thick, cold, snow-free ice. Our fitted value of 0.65 therefore corresponds to the upper end of the observed range for bare ice, while also remaining consistent with Charnay et al. (2013). We have revised the manuscript accordingly:

Ln 174: … following Eq. (3). We calibrate ***the maximum bare sea ice albedo*** *$A_{\text{ice}}^\text{max}$ by fitting this expression to long-term observations of Antarctic sea ice albedo, as documented by \citet[][filled symbols in Fig.\ref{fig:albedo_parameterisation}]{brandt2005surface}, and summarised by \citet{pedersen2009new}.* ***Based on Brandt et al. (2005; Table 3), the VIS (NIR) albedos of bare first year sea ice typically range from $\sim$0.54 (0.27) for thinner ice up to $\sim$0.67 (0.31) for thicker, cold, snow-free ice. Fitting Eq. (3) to these data yields*** ~~*From this, we obtain*~~ *$A_{\text{ice}}^\text{max} \approx 0.65$ in the VIS and ≈ 0.31 in the NIR.*

6. Ln 177: Additional explanation could be added to justify the choice of h_ice,0=0.3 m, which is different from the previously adopted value by Charnay et al. (2013).

The (fitting) parameter h_ice,0 governs the rate of transition between the minimum and maximum albedo values. Since the minimum albedo of sea ice has been changed with respect to Charnay et al. (2013), but the maximum albedo remains the same, the original value of h_ice,0=0.5 m is no longer optimal. We therefore refit this to the observations of Brandt et al. (2005), which yielded h_ice,0=0.3 m. We have clarified this as follows:

Ln 177: The parameter h_{ice} denotes sea ice thickness (in m), while h_{ice}^0 is a scaling parameter ~~*(set to 0.3 m)*~~ *that governs the rate of transition between the minimum and maximum albedo values.* ***Since our formulation differs from that of \citet{charnay2013exploring} in both the minimum albedo (now fixed to the ocean albedo) and in its spectral dependence, the original value of $h_{\text{ice}}^0 = 0.5$ m is no longer optimal. We therefore refit Eq.~(\ref{eqn:albedo-equation}) to the \citet{brandt2005surface} observations, yielding $h_{\text{ice}}^0 = 0.3$ m. The older would still preserve the maximum albedo for thick ice, but would systematically underestimate albedos at intermediate thicknesses.***

7. Ln 183: The choice to adopt the mixed snow profile can be clarified. Here, it is motivated by the fact that it is representative of the albedo of snow-covered sea ice. Is another value chosen for snow on land? Or is the mixed snow profile used for all cases?

The mixed snow spectral albedo profile is used globally in the model, both for snow on land and for snow-covered sea ice. Since the current model does not include a treatment for snow ageing, the mixed snow profile is adopted as a physically reasonable intermediate. We now explicitly state this:

Ln 182: "Currently, our model does not account for an age-dependent snow albedo ***or impurity accumulation****.* ~~*Nevertheless, like \citet{turbet2016habitability}, we adopt the mixed snow profile as it is a representative average of the albedo of snow-covered sea ice.*~~ ***We therefore adopt the mixed snow spectral albedo profile, for both snow on land and for snow-covered sea ice, following \citet{turbet2016habitability}. The corresponding value for Sun-like stars (0.65) is consistent with the mean of the snow and ice albedos (0.8 and 0.5 respectively) reported in Joshi & Haberle (2012). The mixed snow profile also represents a physically reasonable intermediate state between fresh clean snow and old dusty snow, and can be interpreted as a climatological average snow albedo. The pure snow profile would overestimate the strength of the ice-albedo feedback, while the dusty snow profile would underestimate it (see Fig.~\ref{earth-zon-avg} for more details).*** *The dashed lines* ***in Fig.~\ref{fig:albedo_parameterisation}b*** *indicate the normalised black body emission of the Sun (orange, 5778 K), Proxima Centauri (red, 3000 K), and TRAPPIST-1 (brown, 2550 K). For these stars, the bolometric albedo of mixed snow is approximately 0.55, 0.36 and 0.29 respectively\footnote{Assuming blackbody emission is a weak assumption for M-dwarfs, which exhibit significant absorption features.}, highlighting the importance of including a spectral energy distribution in determining surface energy budgets."*

8. Ln 215-222: The transition to a Sverdrup balance seems to be the authors' refinement to the wind-driven Ekman transport implemented in the model already detailed in Codron (2012). However, an assessment regarding how this new development improves the simulation(s) results is missing from the manuscript. The sensitivity of the upwelling structure to the value of epsilon has been discussed in Codron (2012), with repercussions on tropical SST and precipitation. Ln 396-397 specify that lower values of epsilon extend the equatorial cold tongue, but don't specify how the newly implemented Sverdrup balance may improve the results.

We thank the referee for this very valuable suggestion, which motivated us to run additional simulations to clarify the role of the Sverdrup balance. To assess its impact, we ran two new simulations with Sverdrup transport disabled, using different initial conditions to test robustness. The results emphasised the stabilising negative feedback influence of the Sverdrup balance on OHT. Since the manuscript already included a discussion of how OHT mitigates hemispheric climate asymmetries (Section 5.2), we append this section with a new discussion and figures presenting the Sverdrup sensitivity experiments, while removing the final paragraph to avoid redundancy. We also make a minor modification to the Conclusions to explicitly reference the role of the Sverdrup balance. The corresponding changes are detailed below.

Ln 513: … and maintaining a physically realistic climate state.

In our model, this stabilising effect of OHT is largely driven by the wind-curl-sensitive Sverdrup balance implemented near the equator (Section 2.3.1). To assess the impact of this scheme, we conducted two simulations with Sverdrup transport disabled, one

initialised from the converged Case 7 (non-oblique) state, and the other from an isothermal 290 K start to check for dependence on the start state.

Without the Sverdrup balance, near-equatorial OHT responds purely through frictional transport (see Eq. 4). In this case, the cross-equatorial OHT occurs in the same direction as the surface wind. This generates an SST asymmetry (FIGURE sverdrup-off-zonal-map (a)) that shifts the ascending branch of the Hadley cell, thereby amplifying the cross-equatorial wind anomaly (APPENDIX FIG. sverdrup-wind-maps (a)). This leads to a strong hemisphere-wide dichotomy of temperature anomalies (FIGURE sverdrup-off-zonal-map (b)). Moreover, our two Sverdrup-off experiments converge to opposite asymmetric states, illustrating this bistability (FIGURE sverdrup-off-zonal-map (a)).

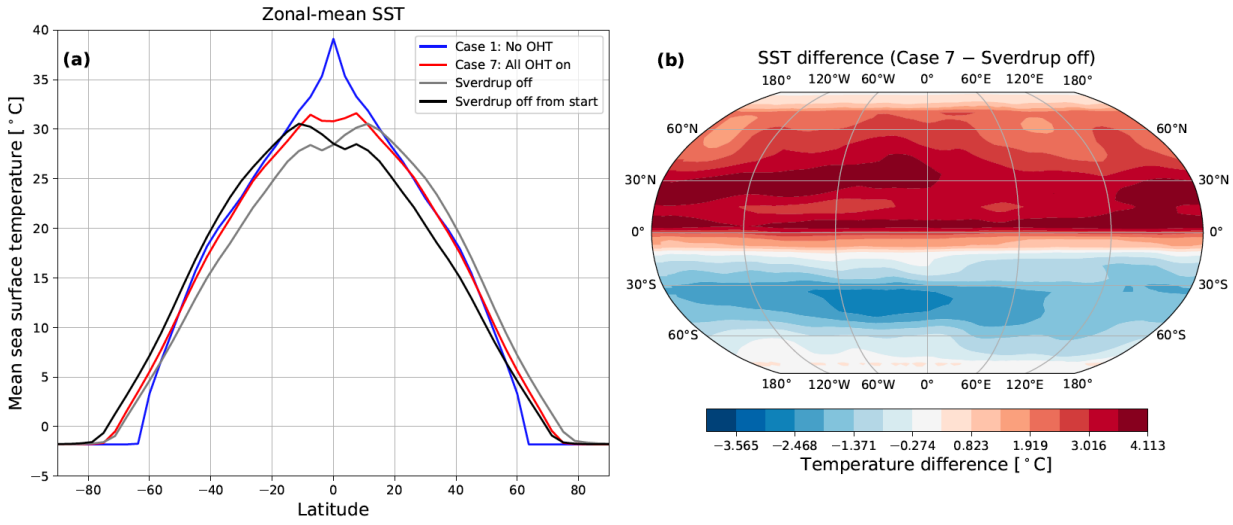

With the Sverdrup balance enabled (Case 7), the near-equatorial transport responds to the wind stress curl rather than its frictional meridional component. For hemispherically symmetric forcing, the wind stress curl remains symmetric about the equator. Importantly, the resulting cross-equatorial OHT occurs opposite to the surface wind direction, introducing a negative feedback that suppresses growing inter-hemispheric asymmetries. As a result, the coupled system converges to a more symmetric equilibrium, both for SST (FIGURE sverdrup-off-zonal-map (a)) and net surface winds (APPENDIX FIG. sverdrup-wind-maps (b)).

Consequently, the inclusion of the Sverdrup balance in our model plays a crucial role in preventing the locking-in of hemispheric biases and maintaining a physically consistent climate.

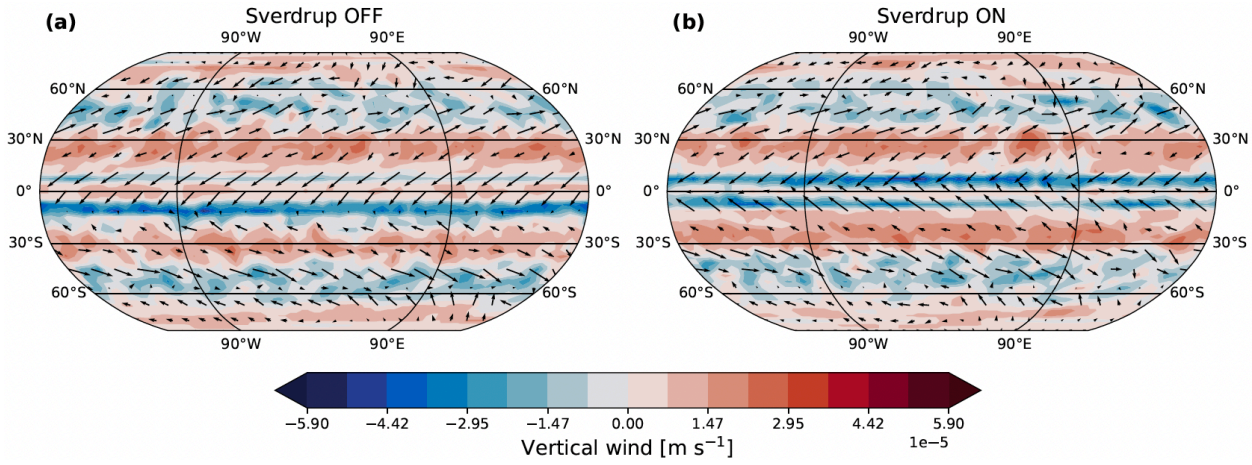

Ln 514-521: With further experiments …… in the model's dynamical core.

Ln 522-525: ~~Altogether, our findings …… in Chaverot et al. (2023) – are present.~~

*Ln 638: Additionally, OHT**, driven particularly by the Sverdrup balance, stabilises the overall climate response and** reduces hemispheric asymmetries that may arise from initial condition biases (Figs. 10 **and XX**~~) and in general, improves model numerical stability~~.*

9. Ln 292: Comments about the discrepancy in spin up times between this work and Codron (2012) would be useful. An upper limit of 40 years, instead of 20 years in Codron (2012) seems non-negligible. The reader would benefit from this comparison, that would highlight which model is more suited to the reader's needs.

The spin up timescale depends on the initial distance of the system from the basin of attraction. Codron (2012) initialised the model from an *idealised* meridional temperature profile (Section 3) with a cosine dependence on latitude (QOBS profile; Neale & Hoskins 2001). We, however, begin from an *isothermal* 290 K state, which is farther from equilibrium, requiring a higher spin up time. When we initialise the model from an idealised meridional profile such as in Codron (2012), our equilibrium is also reached within 15-20 years. We have clarified this point as follows:

*Ln 292: "~~Given the warm start, our~~**The** model typically achieves a steady state within 20~~-40~~ **years when launched from an idealised meridional temperature profile (as in Codron, 2012; similar to the QOBS profile from Neale & Hoskins 2001), and within** 40 years **when initialised from an isothermal 290 K state**."*

10. Figure 3: In this plot, only Case 1 and Case 7 can be compared. A comparison with the aquaplanet results by Codron (2012), without the model improvements detailed in this work, would help clarify why these improvements are significant. When including OHT, Codron (2012) seems to reproduce a flatter SST compared to the one shown in Figure 3a. At the same time in Codron (2012), including OHT moves the mid-latitude storm tracks poleward, while it does not affect their position in Figure 3b. For instance, this comparison could be done through a direct overlay on the plot.

We have added an overlay figure and an accompanying discussion in Appendix~XX. We chose to include these in the Appendix rather than in the main text so that the focus is on the impact of introducing OHT in the main text. Appendix~XX is an appropriate place for the discussion below as it addresses comparisons with Codron (2012). We clarify that a direct attribution of differences in SST flatness and storm-track positions is complicated by substantial changes in the atmospheric model over the past 12-13 years, which already lead to large differences in the OHT-off configurations. Text has accordingly been added:

Ln 674: ***"Appendix F: Comparison with Codron (2012)***

Direct overlays of SST and precipitation profiles:

Interpreting the relative positions of features in the SST and precipitation profiles between Codron (2012) and the present study, and attributing them to specific physical mechanisms, is challenging due to substantial evolution in the GCM (including its atmospheric model) between the two implementations. This is already evident when comparing the OHT-off configurations, which isolate the atmospheric component: the zonal-mean SST profiles in Fig.~XXX(a) (solid and dashed blue lines in this work and Codron (2012), respectively) differ markedly between the two studies.

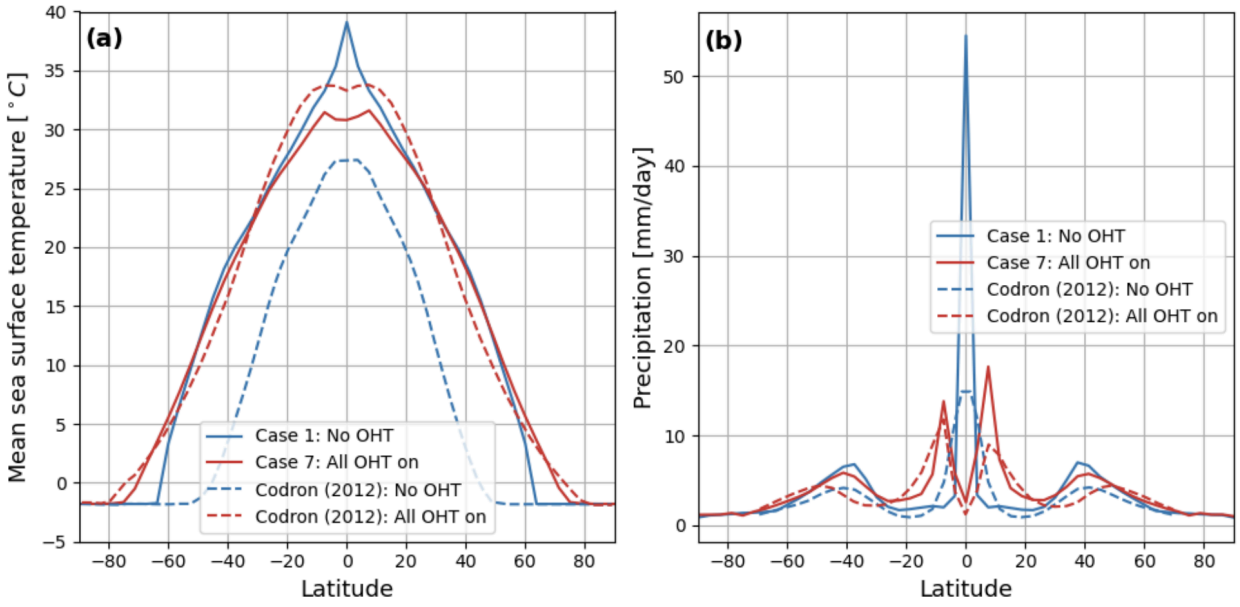

The large difference in equatorial temperatures in the OHT-off cases Fig.~XXX(a) directly affects the magnitude of the equatorial precipitation maxima (Fig.~XXX(b)). In Codron (2012), enabling OHT leads to a slight poleward shift of the storm tracks relative to the OHT-off case. A similar modest shift is observed in our study. However, it is unclear whether this reflects a physical response or a resolution-related artefact.

More generally, differences in profile shapes between Codron (2012) and this study likely reflect differences in atmospheric physics, particularly cloud / precipitation parameterisations, as well as the resolution (leading to stronger / weaker baroclinic

eddies). These combined effects complicate direct one-to-one comparisons of individual climatic features."

11. Figure 5: Again, for this plot a more direct comparison with Codron (2012) would be useful, especially given the evident differences for the Ekman transport in the mid latitudes. For instance, this comparison could be done through a direct overlay on the plot.

We have added an overlay of the corresponding transport components and a related discussion in the manuscript. We show that the similar diffusive transport reflects comparable tuning, while the larger Ekman transport in the present model arises from GM-induced restratification. The revised text and figure have been added.

Ln 340: "... surface wind forcing. Ekman transport (~~black~~ ***solid green*** *line) is strongest in the tropics, consistent with…"*

Ln 345: "... (see Sect. 5.2 for more details).

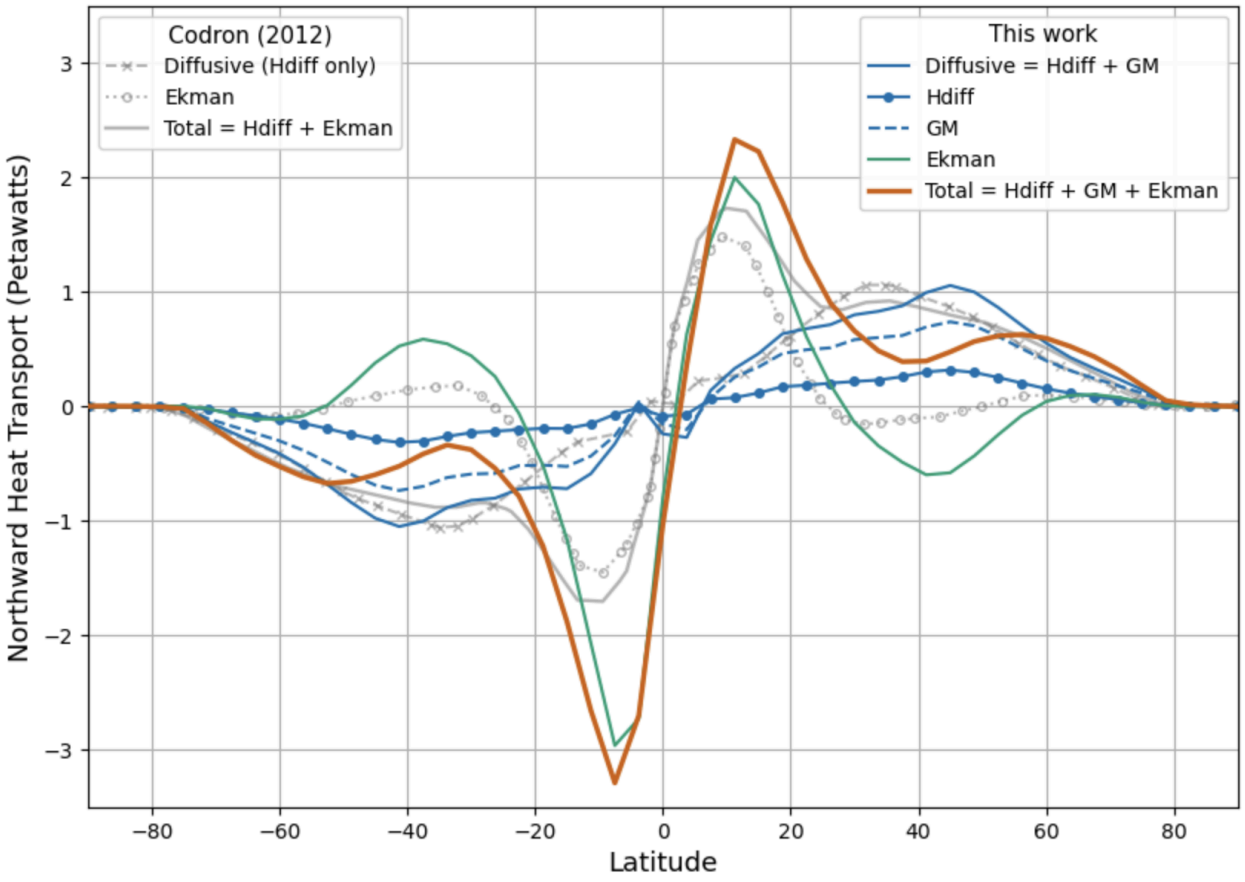

For a more direct comparison, we also overlay the corresponding meridional OHT components from Codron (2012) in Fig.~XX. The total diffusive transport in the mid-latitudes (crossed grey lines in Codron, 2012; solid blue line in this work) is similar in both studies since the diffusion coefficients were tuned toward the same aquaplanet benchmark \citep{marshall2007mean}. *We* ***further*** *decompose the diffusive*

transport… … to the same amplitude as that seen in \cite{codron2012ekman}. ***In contrast, Ekman transport in this work (solid green) exhibits larger amplitudes than in Codron (2012; grey circle-dotted line), in both the tropics and mid-latitudes, reaching values closer to the Eulerian ones in \citet{marshall2007mean}. This difference primarily arises due to GM transport in the present model. In addition to transporting heat downgradient, GM restratifies the two-layer ocean and strengthens Ekman transport. The poleward shifts of the mid-latitude Ekman trough and diffusive peak relative to Codron (2012) likely reflect differences in the atmospheric circulation between the two model versions, which influence surface wind stress and, in turn, OHT profiles.*** *With all components accounted for…"*

12. Ln 354: The general amplitude of the total ocean heat transport in Marshall et al. (2007) does not seem to match what is observed here. In Figure 7 of Marshall et al. (2007), the peak value for OHT exceeds ~4PW, basically double the peak value in this work. This is somewhat similar to the OHT peak values shown in Wu et al (2021), while Brunetti et al. (2019) exhibits lower values.

In Fig. 7 of Marshall et al. (2007) the Eulerian (wind-driven) component exceeds 4 PW, but their total OHT peaks only slightly above 3 PW, which is close to the values obtained here. The larger Eulerian peak in their fully dynamic GCM results from a colder deep return flow, which increases the vertical temperature contrast and therefore, Ekman transport efficiency. This is then partly compensated by an equatorward eddy contribution (~1 PW), yielding a total transport comparable to ours. Our two layer slab ocean model cannot represent this detailed vertical structure. Nevertheless, the resulting total OHT amplitude (2.25–3.25 PW) and latitudinal structure remain comparable to Marshall et al. (2007) and Wu et al. (2021). We have clarified this point in the revised manuscript to emphasise first-order consistency rather than numerical equivalence.

Ln 352: "With all components accounted for, ~~the overall transport (red line), which contributes to the large-scale ocean circulation, resembles those observed on Earth (Trenberth and Caron, 2001). Furthermore,~~ the general amplitudes ***resemble those of*** *~~agree well with aquaplanet results using~~ a full AOGCM (see Figs. 7****, 3, 12*** *and ~~3~~* ***2*** *in Marshall et al., 2007~~;~~****, Wu et al. 2021 and Ragon et al., 2022,*** *respectively)****, despite the much simpler ocean formulation and spatial resolution used here. While the Eulerian (wind-driven) component in Marshall et al. (2007) reaches values exceeding ~4 PW, their total OHT peaks only slightly above ~3 PW. The larger Eulerian peak in fully dynamic models arises because the return flow occurs at greater depths and lower temperatures, increasing the vertical temperature contrast and thereby enhancing the efficiency of Ekman transport. This is then partially compensated by equatorward eddy transport. Our two-layer framework cannot represent this detailed vertical structure; nevertheless, achieving peak transports of 2.25–3.25 PW (solid red line in Fig.XXX) with comparable latitudinal structure indicates that the model captures the first-order behaviour of large-scale OHT. This***

also represents a clear improvement over the peak transport of ~1.75 PW reported in Codron (2012; solid grey line)."

13. Ln 365: As stated previously, comments about the discrepancy in spin up times between this work - 70 years - and Codron (2012) - 10-30 years - would be useful.

The same explanation as that given to question (#9) for the aquaplanet is applicable here. The spin up timescale depends on the initial distance of the system from the basin of attraction. Codron (2012) initialised the Earth simulation also from an *idealised* zonal mean SST (Section 4) following the QOBS profile from Neale & Hoskins (2001). In contrast, we begin from an *isothermal* 290 K state, which is farther from equilibrium, requiring a higher spin up time. We have clarified this point as follows:

Ln 352: "... while that with OHT takes around 70 model years to converge. ***This spin-up time reflects our use of an isothermal 290 K initial state, whereas Codron (2012) initialised the simulations from an idealised meridional temperature profile following Neale & Hoskins (2001).***"

14. Figure 6: A few comments regarding the similarities/differences between this work and previous ones are included. Once again, more cohesive direct comparisons – such as with difference map plots - would highlight what this new version of the model can achieve. For instance, the position of the Pacific cold tongue is more central in Codron (2012) and shifted eastward in this work. An explanation for the shift in the position of the ITCZ is provided in the text.

We thank the referee for this comment. Although a pixel-by-pixel difference map with Codron (2012) is difficult due to data availability, we now discuss the physical origin of the shifted cold tongue position. We attribute this to the introduction of a Sverdrup balance near the equator, which suppresses strong frictional cross-equatorial Ekman flow. We also relate this behaviour to the sensitivity to the friction parameter ε discussed in Codron (2012). We accordingly modify the following lines:

Ln 387: "... evident in observations (for e.g., Cromwell, 1953; Wyrtki, 1966). ***Our more eastward position of the cold tongue compared to Codron (2012) is likely a consequence of Sverdrup dynamics. Codron (2012) used a purely frictional Ekman balance at the equator, and noted that the position of the cold tongue is sensitive to the frictional damping coefficient ε (see Sect. 2.3.1), with lower values of ε favouring an equatorially centered, zonally extended cold tongue. In our study, the introduction of a Sverdrup balance near the equator suppresses unrealistically strong cross-equatorial frictional transport (see Sect.~\ref{subsec:hemisphere-asymmetry} for more details), shifting the equatorial circulation into a curl-driven regime and anchors the upwelling more strongly to the eastern basin.*** *Meanwhile, mid-latitude SSTs are warmer…"*

15. Ln 418: The Southern hemisphere OHT is more severely underestimated than suggested, as "similarly" would imply an equivalent misrepresentation.

We accordingly modify the relevant sentence for better clarity:

Ln 418: "... and Southern Hemisphere OHT is ~~similarly~~ ***also*** *underestimated (-0.3 PW vs. -1.5 PW)…"*

16. Ln 449: These estimates of planetary bond albedo represent an improvement with respect to the 0.36 value in Charnay et al. (2013), and this could be highlighted, especially since the importance of accurately modelling albedo and OLR for exoplanetary studies is mentioned in Ln 468.

We thank the referee for highlighting this. We added text noting that the planetary bond albedo obtained here (≈0.32–0.33) is a clear improvement over the 0.36 value in Charnay et al. (2013). We also modify the reanalysis albedo value from 0.30 to 0.31 following the TOA-bias-corrected values from NCEP/NCAR Reanalysis R-1:

Ln 449: "… in our OHT-on and -off simulations, is approximately 0.32 and 0.33, respectively, closely matching the ~~observed~~ value of ~~0.30~~ ***0.31*** *derived from* ***the*** *NCEP/NCAR ~~reanalyses~~* ***Reanalysis R-1. These represent a substantial improvement over the value of 0.36 obtained in Charnay et al. (2013), who attributed their high albedo value to an excessive amount of clouds produced at the ITCZ. Our lower and more realistic albedo therefore suggests that we have a reduced ITCZ cloud bias, although a detailed cloud radiative analysis is beyond the scope of this work.****"*

17. Ln 464: The discrepancy between the global annually averaged surface temperature in this work (13°C, NCEP/NCAR reanalysis 14.0°C) and Charnay et al. (2013) (14.9°C, NCEP reanalysis 15.0°C) can be potentially discussed.

We discuss the likely origin of the difference between the global annually averaged surface temperature obtained here and in Charnay et al. (2013). We explain that Charnay et al. (2013) obtained a warmer climate due to a combination of stronger meridional heat transport, enhanced greenhouse effect from high clouds and the seasonal disappearance of Arctic sea ice, whereas in our simulations Northern Hemisphere sea ice is retained year-round, contributing to a slightly cooler high-latitude climate. The corresponding text has been added in two places in that section:

Ln 452: "... closer to the observed range (18-27 million km2) than the OHT-off case. ***Additionally, in contrast to Charnay et al. (2013), we retain Northern Hemisphere sea ice throughout the year, whereas in their setup it disappeared completely in the summer.*** *However, both****, our OHT-on and -off cases still*** *~~model versions~~ overestimate Northern Hemisphere sea ice…****"***

Ln 464: "... In contrast, the simulation without OHT yields a cooler average temperature of 12°C. ***Charnay et al. (2013), by comparison, obtained a warmer OHT-enabled mean temperature of 14.9°C. They note that this likely results from a combination of an overly strong meridional heat transport and an enhanced greenhouse effect due to a larger amount of high clouds, as well as the seasonal***

disappearance of Arctic sea ice in summer. In our work, Arctic sea ice is retained throughout the year, which contributes to a slightly cooler climate."

18. Ln 480 (but this is a more general comment regarding the impact of GM on all analysed quantities): Comparing the cases Hdiff+Ekman+GM(+conv.) and an additional case Hdiff+Ekman+conv. would be especially interesting in order to clarify the importance of including GM. When excluding GM (like in Codron (2012)), does convective adjustment dominate? In other words, if including all other processes, does including/discarding GM have a significant impact on the state of the climate? Moreover, regarding the need for a detailed comparison with previous versions of the model, Hdiff(8000m2s-1)+Ekman+GM+conv. should be compared to Hdiff(25000m2s-1)+Ekman+conv.. Assessing whether convection and horizontal diffusion can effectively substitute GM is required to have a clearer understanding of why distinguishing different processes might be necessary. Given that the parameterization of GM in this model is one of the main proposed improvements, this question needs to be addressed.

We thank the referee for this suggestion. We address this comment in three parts:

First, to clarify the importance of including Gent–McWilliams (GM) advection relative to convective adjustment, we performed additional aquaplanet simulations explicitly comparing cases with horizontal diffusion and Ekman transport plus convective adjustment, both with and without GM, as well as a sensitivity test with a larger GM transfer coefficient. These new results are presented and discussed in Section~\ref{subsec:gm-discussions}. We find that convective adjustment alone does not reproduce the equilibrium climate obtained when GM is included: even when convection is active, adding GM leads to systematic cooling of the deep ocean by 2–4°C at mid-latitudes. Conversely, when GM is already present, adding convective adjustment produces only minor additional changes. Accordingly, the section title has been changed to "The role of the Gent-McWilliams scheme: Influence on vertical structure and ocean heat transport" Figure 9 has also been modified with 2 additional subplots. The section has been rewritten as follows:

Ln 475: "One of the additions to the Generic-PCM's dynamical slab ocean model is the Gent-McWilliams (GM) parameterisation \citep{gent1990isopycnal}. The GM scheme enables isopycnal mixing ~~allowing for temperature diffusion across ocean layers and reducing excessive vertical temperature gradients~~ ***and modifies the large-scale ocean temperature structure (Fig.~\ref{fig:deep-layer-temperature-Dec2025}) through horizontal and vertical heat redistribution****. ~~While this mixing tends to decrease stratification, it still modifies the temperature contrast between the surface and deeper layers that drives Ekman transport. As a result, the GM parameterisation introduces a two-way interaction between eddy-induced and wind-driven circulation, even within our idealised setup.~~* ***In our two-layer model, this redistribution alters the temperature contrast between the surface and deep layers that drives Ekman transport (see Section 2.3.1), thereby introducing a coupling between eddy-induced and wind-driven circulation.***

Figure 9 Caption: *Gent-McWilliams (GM) restratification ~~mimics the effect of convective adjustment:~~**relative to convective adjustment:** Zonally averaged deep ocean layer temperatures in the aquaplanet simulations. ~~(a)~~ **Top panels:** Mean deep layer temperature (in $^\circ$C) for cases ~~including horizontal diffusion and Ekman transport (blue), with the addition of GM (black), and finally with convective adjustment (red).~~ ~~(b)~~ **Bottom panels:** Differences between selected simulations.

~~*Interestingly, we find that the restratification produced by the GM scheme plays a role analogous to convective adjustment. Figure~\ref{fig:deep-layer-temperature}a shows the decadal-averaged zonal deep layer temperatures for three aquaplanet simulations. Case 6 (black line), which includes horizontal diffusion, Ekman transport and GM, is nearly indistinguishable from Case 7 (red line), which also includes convective adjustment. This lack of difference indicates that convective processes contribute negligible additional transport in this configuration. In contrast, Case 4 (blue line), which excludes GM, exhibits significantly warmer deep layer temperatures at mid-to-high latitudes. Figure~\ref{fig:deep-layer-temperature}b, which presents temperature differences between simulations, highlights this: the inclusion of GM cools the deep ocean by 3–7°C in high-latitude regions, whereas adding convection yields negligible change. These results suggest that under the tested conditions, GM alone captures the dominant effects typically associated with convective adjustment – namely, vertical mixing in regions of unstable stratification. Although our GM scheme was designed to parameterise mesoscale eddies along isopycnals, it also implicitly induces vertical mixing and thereby mimics convection.*~~

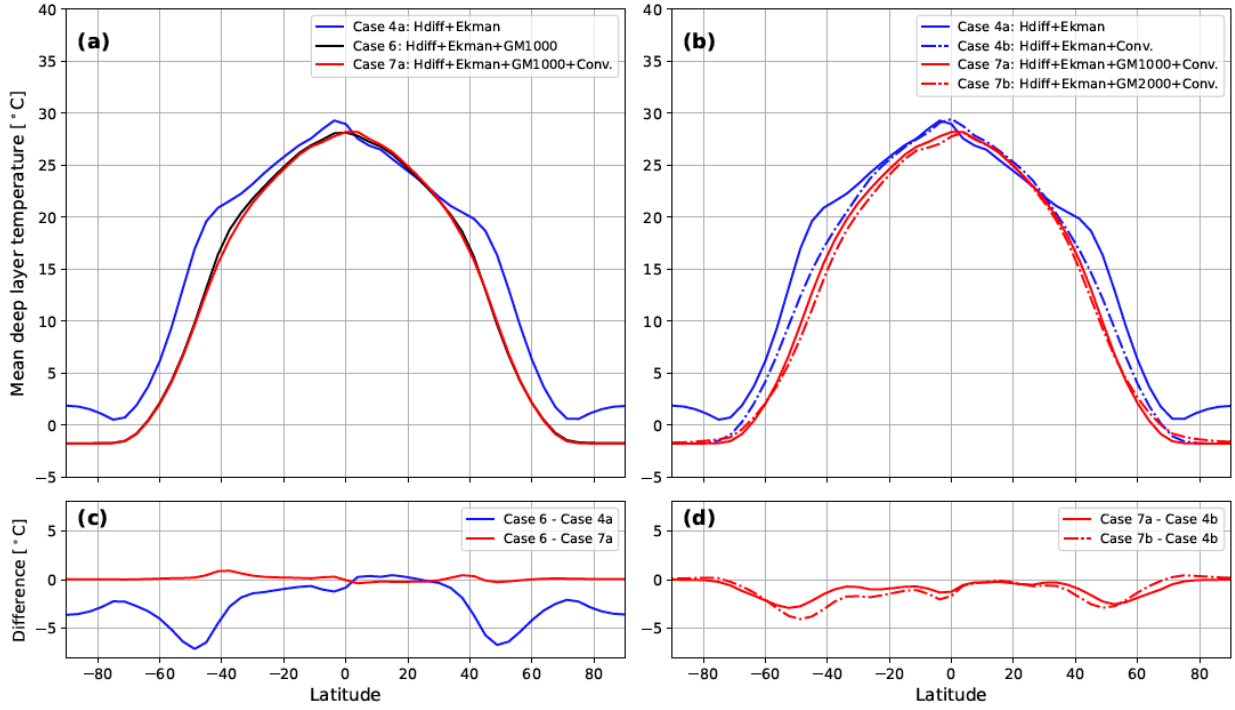

To assess the relative importance of GM and convective adjustment, we compare a hierarchy of aquaplanet simulations that systematically include or exclude these

processes. Figure~\ref{fig:deep-layer-temperature-Dec2025}a shows the decadal-averaged zonal deep layer temperatures of the relevant simulations. Case 6 (horizontal diffusion + Ekman + GM; solid black line) exhibits substantially cooler deep layer temperatures at mid- to high latitudes than the simulation without GM, Case 4a (horizontal diffusion + Ekman; solid blue line), with differences reaching 5–7°C (see Fig.~\ref{fig:deep-layer-temperature-Dec2025}c). In contrast, adding convective adjustment on top of GM (Case~7a; solid red line) produces only negligible additional changes (Fig.~\ref{fig:deep-layer-temperature-Dec2025}c). This indicates that, under the conditions tested here, the inclusion of GM substantially modifies vertical stratification such that convective adjustment contributes little further modification to deep layer temperatures.

We next consider Case 4b (horizontal diffusion + Ekman + convective adjustment; dash-dotted blue line). Compared to Case 4a, convective adjustment reduces the deep layer temperatures (Fig.~\ref{fig:deep-layer-temperature}b), but this cooling is weaker than that produced by only GM (Fig.~\ref{fig:deep-layer-temperature-Dec2025}c). Still, this highlights that the effects of GM and convective adjustment are not simply additive. To further isolate the role of GM when convective adjustment is already active, we compare Case 4b with Case 7a. This reveals that the inclusion of GM, which drives eddy-induced heat redistribution, produces additional mid-latitude cooling of 2-3°C (Fig.~\ref{fig:deep-layer-temperature-Dec2025}d). This shows that GM has a distinct influence on the deep ocean even in the presence of convective adjustment.

To test sensitivity to the strength of GM, we performed Case 7b, in which the GM transfer coefficient is increased to 2000~m^2~s^{-1} (compared to 1000~m^2~s^{-1} in Case 7a). Due to the increased coefficient, mid-latitude cooling reaches 3-4°C (Fig.~\ref{fig:deep-layer-temperature-Dec2025}d), consistent with stronger eddy-induced redistribution of heat. This could be particularly relevant for slowly rotating planets, for which effective GM coefficients could be substantially larger. This will be investigated in future work.

Overall, these results show that convective adjustment alone does not reproduce the equilibrium climate obtained when GM is included. Even when convection is active, adding GM leads to systematic cooling of the deep ocean at mid-latitudes, whereas adding convective adjustment to a configuration that already includes GM produces only minor additional changes.”

The second aspect raised was to check if horizontal diffusion and convective adjustment can substitute for GM. For this, we performed additional simulations comparing a Codron (2012)-style configuration (horizontal diffusion coefficient of 25000~m^2~s^{-1}, Ekman transport and convective adjustment) with the recommended configuration of the present model including GM. To enable a meaningful comparison, we also repeated the Codron-style setup with the Sverdrup balance enabled. Our results show that even with substantially increased horizontal diffusion and active convection, the absence of GM leads

to systematically warmer mid-latitude deep-layer temperatures. This demonstrates that horizontal diffusion and convective adjustment do not fully reproduce the effects of GM. Below are the relevant additions to the manuscript, first, the brief addition to the above section, followed by a detailed analysis in Appendix~X:

Ln 490+: ***"... includes GM produces only minor additional changes.***

This is further emphasised in another set of simulations to assess whether an enhanced horizontal diffusion and convective adjustment can substitute for GM. For this, we compared a Codron (2012)-style configuration (horizontal diffusion coefficient of 25000~m^2~s^{-1}, Ekman transport and convective adjustment) with the recommended configuration of the present model including GM. Our findings show that even with substantially enhanced horizontal diffusion and active convection, the absence of GM leads to systematically warmer mid-latitude deep-layer temperatures. This comparison is discussed in detail in Appendix~F."

Ln 674: ***"Appendix F: Comparison with Codron (2012)***

Direct overlays of SST and precipitation profiles:

Interpreting the relative positions …

… one-to-one comparisons of individual climatic features."

Vertical ocean structure:

It is important to assess whether the improvements obtained with the present model configuration reflect the inclusion of GM transport, or whether similar behaviour could be achieved with an enhanced horizontal diffusion coefficient (25000~m^2~s^{-1}), Ekman transport and convective adjustment, like in Codron (2012). We compare this configuration with the recommended ocean setup of the present model, which employs a smaller horizontal diffusion coefficient (8000~m^2~s^{-1}), GM transport (2000~m^2~s^{-1}), Ekman transport and convective adjustment.

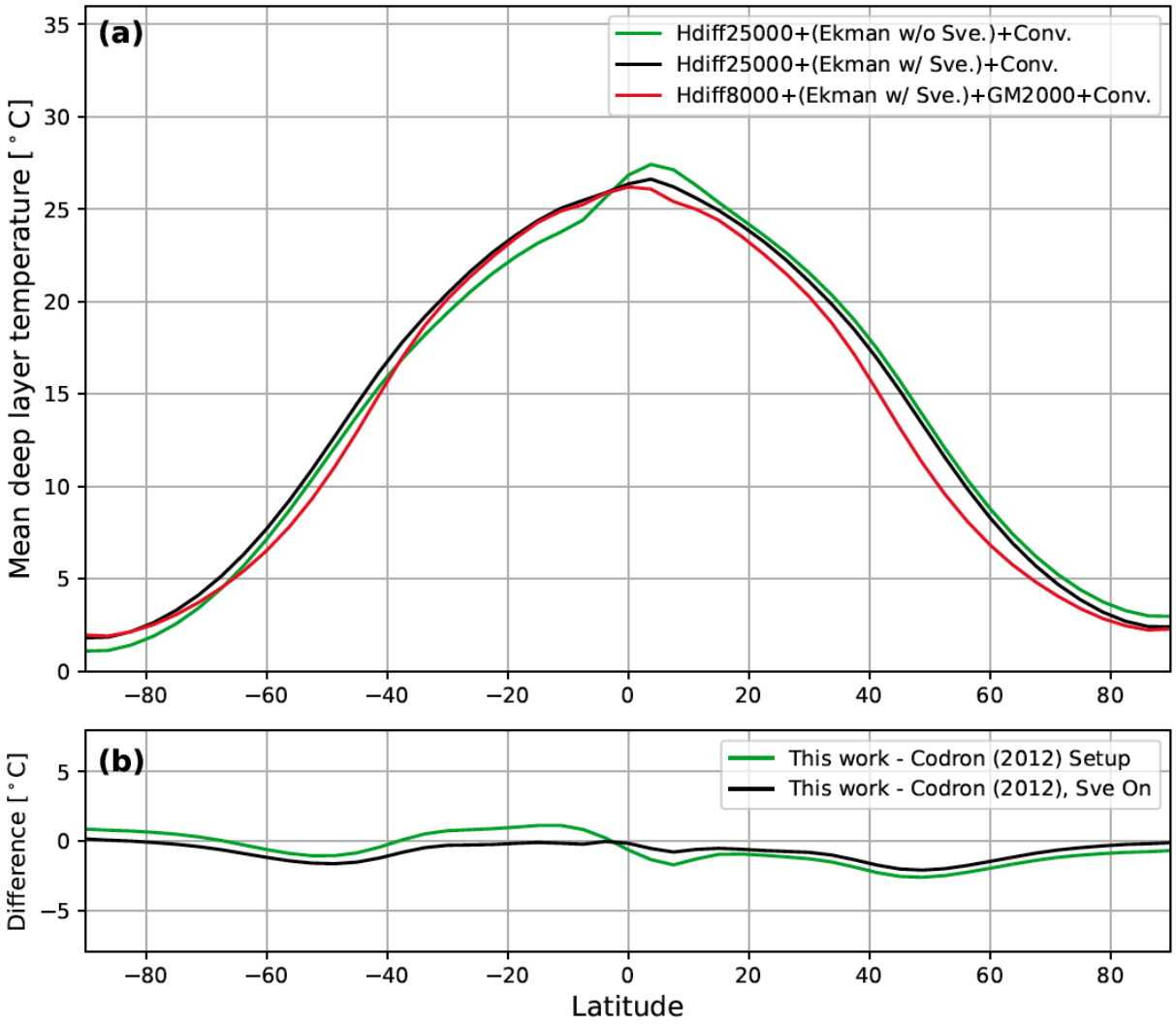

Figure~\ref{fig:deep-layer-temperature-comparison-Codron}a shows the zonally averaged deep layer temperature profiles for the tested configurations. Comparison with the Codron (2012) configuration (green line) is complicated by the pronounced hemispheric asymmetry that now develops in the absence of the Sverdrup balance, as explained in SECTION X. To isolate the effects of the parameter choices, we perform a simulation using the Codron setup but with the Sverdrup balance enabled (black line). We see that both these Codron-style configuration(s) produce(s) systematically warmer deep layer temperatures at mid-latitudes than the present configuration with GM (red line). The difference of the Codron (2012) configurations with the current recommended setup is shown in Figure~\ref{fig:deep-layer-temperature-comparison-Codron}b. Here, we see that the simulation with GM transport is approximately 2°C cooler in the mid-latitudes (black line). This comparison again demonstrates that neither enhanced horizontal diffusion nor convective adjustment alone can fully reproduce the thermal structure

obtained when GM is included. It further indicates that by modifying large-scale stratification, GM transport exerts a distinct influence on the climate."

Lastly, following your suggestion for a more in-depth comparison with a Codron (2012)-like setup, we have added text in this section comparing the ocean heat transport structure of the present model with that obtained using Codron (2012)-like configurations. It analyses the impact of the Sverdrup balance, Gent–McWilliams transport and updated parameter choices on the total and decomposed OHT, while also placing the results in the context of AOGCM benchmarks:

Ln 490+: ***"... This comparison is discussed in detail in Appendix~X.***

To further contextualise the present model, we compare the OHT structure obtained using the configuration of Codron (2012). Figure~\ref{OHT-profiles-comparison.pdf} presents total and decomposed meridional OHT profiles for three configurations, allowing us to isolate the effects of the Sverdrup balance, Gent–McWilliams (GM) transport and updated parameter choices.

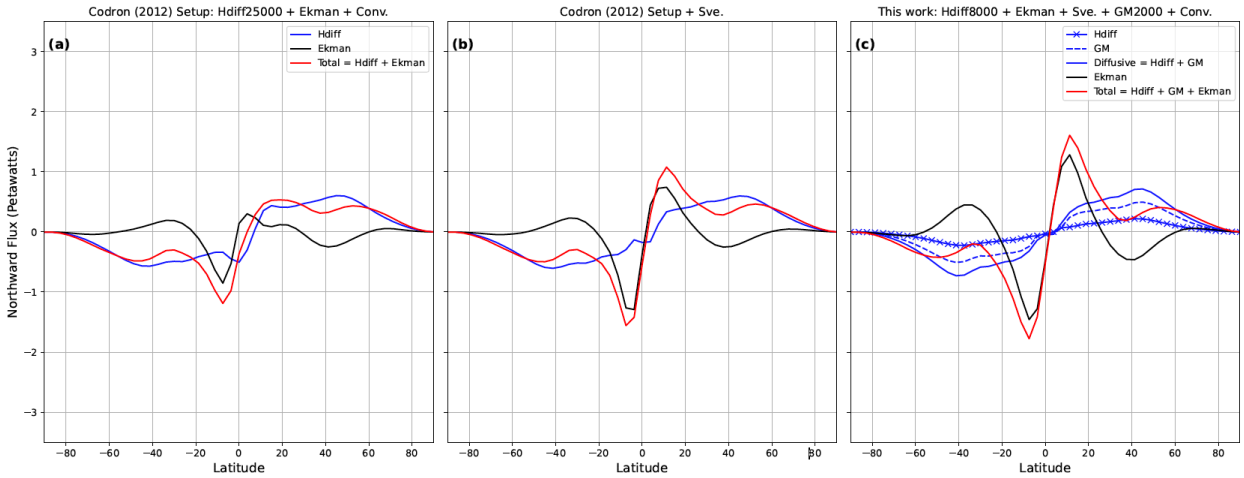

Panel~(a) reproduces the Codron (2012) oceanic configuration as closely as possible, with horizontal diffusion (coefficient of 25000~m^2~s^{-1}), Ekman transport (without the Sverdrup balance) and convective adjustment. In this configuration, the OHT exhibits a pronounced hemispheric asymmetry, discussed in detail in Section~X. Interestingly, the OHT in Fig.~4 of Codron (2012) is quite symmetric, despite the absence of Sverdrup balance in that study. This could point towards a decreased sensitivity of the atmospheric model to surface temperature variations in that version of the GCM. Correspondingly, it implies that the current atmospheric model is either sufficiently or overly sensitive to surface temperature variations. While investigating the related sensitivity is beyond the scope of this work, its physical reasoning is explained in Section~X.

Panel~(b) shows the same Codron-style configuration but with the Sverdrup balance enabled. This largely restores hemispheric symmetry in the OHT, showing its

negative-feedback-induced stabilising role (see Section XXX for more details). However, despite this improvement, the amplitude of tropical Ekman transport remains suppressed relative to AOGCM benchmarks (e.g., Marshall et al., 2007; Ragon et al., 2022). This indicates that the Sverdrup balance alone is insufficient to recover a realistic OHT structure when GM transport is absent.

Panel~(c) presents the recommended oceanic configuration of the present model, which uses a reduced horizontal diffusion coefficient (8000~m^2~s^{-1}), GM transport (2000~m^2~s^{-1}), Ekman transport with the Sverdrup balance, and convective adjustment. Here, the tropical OHT peak – primarily driven by Ekman transport – reaches amplitudes closer to those in fully coupled AOGCM simulations (e.g., Fig.~7 of Marshall et al., 2007; hot-state solutions in Fig.~2 of Ragon et al., 2022) than those obtained either in Codron (2012; Fig. 4) or in the Codron (2012) setups with the current model. This increase arises since GM transport modifies the temperature contrast between the surface and deep layers, thereby affecting the strength of Ekman transport (Eqn.~\ref{eqn:ekman-equation}). Likewise, the Ekman-driven mid-latitude trough is more pronounced due to GM transport in panel~(c), resembling the amplitude of the Eulerian transport component in AOGCM simulations (Marshall et al., 2007; Fig. 7). Compared to the $\sim$30° peak in Fig.~4 of Codron (2012), the latitude of the diffusive transport peak also shifts poleward to approximately 45°, in closer agreement with Marshall et al. (2007). Its peak amplitude (around 0.6 PW) is provided solely by horizontal diffusion in panels (a) and (b). In contrast, the present model decomposes diffusive transport into its horizontal diffusion and GM transport components, yielding a slightly larger combined diffusive peak of $\sim$0.75~PW in panel~(c). The tropical OHT peak is also sensitive to the system's climatic attractor. In panel~(c), which corresponds to a "hot state" (see Brunetti et al., 2019) with no sea ice, the tropical OHT peak is approximately 1.75 PW, consistent with the hot state solution of Ragon et al. (2022; Fig. 2) obtained with the MITgcm. In contrast, in simulations tuned to reproduce an Earth-like sea-ice distribution (e.g., Fig.~5), we obtained peak transports of 2–3 PW, similar to the warm state attractor in Ragon et al. (2022).

These comparisons demonstrate that the combined inclusion of the novel features of the model: Sverdrup balance, GM transport, and updated parameter choices, leads to an improvement over Codron (2012). The resulting OHT structure more closely resembles that of fully dynamic AOGCMs, despite the relative simplicity of our model."

19. Ln 529-531: A q-flux, although certainly not ideal, can be prescribed for already well-studied cases. Analogously, the model presented here can currently only be somewhat accurately applied to cases characterized by well-known parameter values, valid for Earth-like spin states. This is specified throughout the manuscript: the current Sverdrup transport would be unrealistically large for slowly rotating

planets (Ln 223-224), the values for GM diffusion coefficient and maximum slope are tuned to fit AGCM results for aquaplanet with Earth rotation rate (Ln 239-240), the horizontal diffusion coefficient is specific to Earth's rotation (Ln 226-227).

We now explicitly acknowledge that, like q-flux approaches, the current implementation of our dynamical slab ocean model is primarily calibrated for Earth-like rotation rates and parameter regimes. We have added text highlighting that the Sverdrup formulation and diffusion coefficients are presently tuned using Earth-rotation aquaplanet benchmarks, and that extensions to other regimes will be done in the future. Still, we emphasise that a key distinction from q-flux methods is that OHT in our model emerges dynamically and responds interactively to atmospheric forcing. The following lines will be modified as follows:

Ln 531: "… (with some exceptions: for e.g., Del Genio et al., 2019; Yang et al., 2020; Batra and Olson, 2024), ~~*no q-flux can be prescribed*~~ ***a physically motivated q-flux cannot be prescribed.****"*

Ln 539: "… strongly coupled via surface winds. ~~*Unlike q-flux oceans, our approach allows for the ocean to dynamically adjust to evolving atmospheric and external conditions, leading to a more physically consistent climate response.*~~

We note, however, that our current version of the model is primarily designed for Earth-like rotation rates and parameter regimes. For instance, our Sverdrup balance may overestimate transport for slowly rotating planets (Sect.~\ref{subsubsec:ekman-transport}) and diffusion coefficients are calibrated using Earth-rotation aquaplanet benchmarks (see Sects.~/ref{subsubsec:gent-mcwilliams} and \ref{subsubsec:horizontal-diffusion}). Given this, our approach currently shares with q-flux methods a reliance on well-characterised regimes. Nevertheless, a key distinction is that even within these regimes, OHT in our model is not prescribed but responds interactively to changes in atmospheric forcing and climate state. Extending the framework to other planetary contexts is a natural direction for future work.*"***

20. Ln 558-560: Given the stated intention of using the model to simulate exoplanetary climates, I once again recommend implementing a discussion regarding the differences between this work and results previously presented in Codron (2012) and Charnay et al. (2013). In the context of exoplanetary studies, in which observational constraints are mostly uncertain – as stated in the manuscript – does this new refined model present significant improvements in simulating planetary climate with respect to Codron (2012) and Charnay et al. (2013)? While the potential of applying these models is evident, and introducing spectrally dependent refinements for ice and albedo is certainly important, the manuscript does not highlight major advantages regarding this improved version of the model. For instance, Ln 600-603 justify the choice of disregarding the role of salinity, and therefore thermohaline circulation, in shaping climate. This appears to have major impacts on climate in

terms of ocean transport and heat storage (Cullum et al. (2014)) compared to what seems to be a minor implication of including a GM parameterisation in this model.

We agree that the advantages of the present model relative to Codron (2012) and Charnay et al. (2013) should be more clearly articulated in the context of exoplanet applications. We have therefore added a dedicated subsection highlighting the relevant developments, including the spectrally dependent sea ice and snow albedo, the tuning framework that the GM scheme provides, benefits of the new flexible and modular architecture, and the fact that this version of the code is fully parallelised. The corresponding text is shown below:

Ln 560+: ***\subsection{\label{subsec:albedo-gm-sensitivity}Advances over previous dynamical slab ocean implementations}***

We summarise below the key developments of the present model relative to earlier implementations (Codron, 2012; Charnay et al., 2013) that enhance its suitability for exoplanet and paleoclimate applications.

We have two improvements particularly relevant for simulating M-star planets, which are of high interest given their abundance in the galaxy and their observational accessibility. First, the inclusion of a spectrally dependent sea ice and snow albedo (Sect. 2.2) enables more realistic radiative feedbacks on planets receiving non-solar spectra. For M-dwarfs, broadband albedos of snow and ice can be 25–55% lower than for G-type stars (Joshi & Haberle, 2012), making this refinement essential for accurate climate modelling. This is also critically important to better interpret observational data from the JWST and in the future, the ELT.

Second, the introduction of GM transport represents more than a numerical improvement. Through its transfer coefficient, the GM scheme acts as a tuning parameter that controls the effective scale of mesoscale eddies (see Sect.~XXX), enabling exploration of different rotational regimes, notably slow rotators such as TRAPPIST-1e (rotation period 6.1 days) and Proxima b (11.2 days), for which mixing is expected to differ substantially from Earth (e.g., Cullum et al., 2014). In earlier models lacking GM (Codron, 2012; Charnay et al., 2013), no consistent framework existed to account for such regime-dependent mixing.

Another strength of the present framework is its flexible architecture. Individual oceanic processes can be selectively (de)activated through configuration flags, allowing users to isolate processes, depending on the need. Moreover, the modular design enables technically straightforward integration of additional processes, such as a simplified sea-ice drift scheme (see Sect.~XXX), also important for exoplanet applications (Yang et al. 2020).

Finally, the present ocean model is fully parallelised, in contrast to the implementations of Codron (2012) and Charnay et al. (2013). This enables efficient long integrations and large ensemble simulations (see Appendix~X for more details),

which are essential for exoplanet and paleoclimate studies where observational constraints are sparse.

We make a relevant addition taking inspiration from Cullum et al. (2014) to our discussion about the scaling of diffusion coefficients for slow rotating planets. The text has been added to Section~X:

Ln 574: "*... that eddy-driven mixing processes may differ substantially on such climates (see Showman et al., 2010~~, for a detailed review~~ and Cullum et al., 2014).* ***Though we don't have the density-driven component of the MOC, our GM scheme does influence its temperature-driven part, and also leads to high-latitude surface warming and low-latitude depth cooling like what Cullum et al. (2014) showed was the case for slower rotation rates, where they saw an increased MOC strength resulting in high-latitude surface warming and low-latitude depth cooling. This is a strong motivation for us to modify the GM coefficient in future exoplanet implementations of the model."***

We also clarify the rationale for neglecting prognostic salinity as a deliberate trade-off between realism and computational efficiency. The corresponding text has been added to Section~X:

Ln 599: "... vertical mixing. ~~*While including a prognostic salinity field would improve realism and enable the simulation of regional ocean features, it would also significantly increase model complexity.*~~ ***While density-driven circulation due to salinity is important in shaping OHT (e.g., Cullum et al., 2014), its inclusion would substantially increase model complexity and computational cost. In this context, our GM transport scheme provides an intermediate complexity alternative balancing realism and efficiency.*** *For exoplanet studies, where the priority …"*

21. Ln 565: Additionally to geothermal heat fluxes, internal tidal heating (Driscoll & Barnes 2015, Dobos et al 2018) can also be modelled and included. Moreover, in the context of aquaplanets orbiting low-mass stars, ocean tides shape ocean circulation and have significant impact on climate (Di Paolo et al. 2025, Si et al. 2022). Including tidal effects might further improve the model and offer a more realistic depiction of climate in exotic contexts.

We have expanded the subsection to acknowledge internal tidal heating as an additional energy source alongside geothermal heat fluxes. We also now note that tidal forcing of the ocean can influence circulation and climate, and emphasise that these represent promising future extensions of the model:

Ln 565: "… or spatiotemporally varying ground-heating term (see Eq.~\ref{eqn:general-equation}). ***Internal tidal heating may also represent an additional and potentially dominant heat source for some close-in terrestrial exoplanets \citep[e.g.,][]{driscoll2015tidal,dobos2018tidally,bolmont2026}. Furthermore, tidal forcing of the ocean can influence the large-scale circulation and climate, particularly***

for aquaplanets orbiting low-mass stars, where strong tides can significantly influence ocean mixing and heat transport \citep[e.g.,][]{si2022tidal,dipaolo2025tidal}. These additional physical processes represent promising future directions, especially in the context of exoplanetary regimes.”

22. Ln 669: Some additional comparison with AOGCM computation time would be useful. For instance, computation time for the favoured AOGCM ROCKE-3D 2.0 appears to be significantly shorter (Figure 15 of Tsigaridis et al. (2025)), even though timestep frequency is not comparable to this case.

We have expanded the relevant appendix section to clarify that quantitative model comparisons of computation time must be treated with caution as GCM performance depends strongly on timestep choice and other factors. We now explicitly reference the efficiency of ROCKE-3D 2.0 and that of the Generic-PCM’s dynamical slab ocean model.

Ln 669: “... compared to the cost of the atmospheric model and coupling processes.

We emphasise that direct quantitative comparisons of wall-clock computation time between climate models must be interpreted with caution, as GCM performance depends strongly on timestep frequency, model heritage and physical parameterisations, particularly radiative transfer. Fully coupled AOGCMs such as ROCKE-3D~2.0 can, in some configurations, achieve shorter per-model-day computation times; for instance, simulation P2SAoM40 in Tsigaridis et al. (2025) reports a cost of 0.18 minutes per simulated day, compared to around 0.45 minutes per simulated day for our model. However, differences in timestep frequency and in how often ocean and radiative processes are called make direct one-to-one comparisons difficult.

Another important practical consideration is not only the wall-clock cost per simulated day, but the number of model years required to reach equilibrium. In our aquaplanet experiments with OHT enabled, equilibrium is typically achieved within 15–40 model years, depending on the initial state. On 24 cores, this corresponds to convergence within 5 days of wall-clock time. Equilibration times for fully coupled AOGCMs are often approximately hundreds to thousands of model years, implying convergence times ranging from weeks to months.

However, at higher horizontal resolutions, OHT-on simulations …”

RESPONSE TO REFEREE #2

A Fast and Physically Grounded Ocean Model for GCMs: The Dynamical Slab Ocean Model of the Generic-PCM (rev. 3423)

We sincerely thank Referee #2 for their report and constructive criticism. It has been very useful for improving our manuscript. Below, we first provide a response to the general comments and then a point-by-point response. Where appropriate, we indicate how the manuscript will be revised in the final version. We paste the original comments in red and our response in black. Our proposed changes to the manuscript are presented cursive and as separate blocks.

Referee Report (received on 09 Feb 2026)

General Comments

This manuscript showcases and benchmarks an improved 2-layer slab ocean model intended for use in long-running coupled atmosphere-ocean applications. The authors note that the flexibility of the model makes it suitable for studies of paleo-earth, or exoplanets with even more exotic characteristics compared to the modern Earth. The new model combines the computational efficiency of a slab model, with the added realism of ocean heat transport parametrisation schemes. The study is well motivated, argued and written, and all figures and schematics are clear and easy to understand. Some small improvements could be made to improve clarity for the reader, but I overall find the breadth of the study, thorough literature review and depth of the analysis of the model performance and biases to be satisfactory.

Discussion:

It would be good to provide an estimate for how this model compares in computational cost to the ocean GCMs typical for exoplanet study. This would provide a better sense of the cost-benefit of choosing this model over a more complex one.

General comment:

No explicit comparisons are made to the Codron 2012 model, even though this is referenced as something on which this model improves. Is this because turning off the OHT parameterisations in this model result in very similar performance to Codron 2012? If so, this should be stated or argued explicitly. If not, then some comparison with Codron 2012 would strengthen the manuscript.

We thank the referee for the careful and constructive evaluation. We have substantially revised the manuscript to address the points raised.

We agree that a clarification of computation time comparison between this model and typical exoplanet AOGCMs should be provided. We have expanded the relevant appendix section and clarified that quantitative model comparisons of computation time must be treated with caution as GCM performance depends strongly on timestep choice and other factors. We now explicitly reference the efficiency of ROCKE-3D 2.0 (an exoplanet GCM with a fully dynamic ocean model) and that of the Generic-PCM's dynamical slab ocean model.

Ln 669: "... compared to the cost of the atmospheric model and coupling processes.

We emphasise that direct quantitative comparisons of wall-clock computation time between climate models must be interpreted with caution, as GCM performance depends strongly on timestep frequency, model heritage and physical parameterisations, particularly radiative transfer. Fully coupled AOGCMs such as ROCKE-3D~2.0 can, in some configurations, achieve shorter per-model-day computation times; for instance, simulation P2SAoM40 in Tsigaridis et al. (2025) reports a cost of 0.18 minutes per simulated day, compared to around 0.45 minutes per simulated day for our model. However, differences in timestep frequency and in how often ocean and radiative processes are called make direct one-to-one comparisons difficult.

Another important practical consideration is not only the wall-clock cost per simulated day, but the number of model years required to reach equilibrium. In our aquaplanet experiments with OHT enabled, equilibrium is typically achieved within 15–40 model years, depending on the initial state. On 24 cores, this corresponds to convergence within 5 days of wall-clock time. Equilibration times for fully coupled AOGCMs are often approximately hundreds to thousands of model years, implying convergence times ranging from weeks to months.

However, at higher horizontal resolutions, OHT-on simulations …"

In response to the referee's request, we also incorporate more systematic comparisons with Codron (2012) and Charnay et al. (2013) throughout the revised manuscript. These revisions include: (i) direct overlays of temperature, precipitation and meridional ocean heat transport (OHT) components, (ii) dedicated discussion and appendix sections comparing SST structures and OHT decomposition, and (iii) clearer identification of the physical origin of differences, including the roles of the Sverdrup balance, Gent–McWilliams (GM) transport, and updates to the atmospheric model. Since Referee #2 specifically requested for explicit comparisons, only the associated changes for that have been indicated below:

Ln 674: ***"Appendix F: Comparison with Codron (2012)***

Direct overlays of SST and precipitation profiles:

Interpreting the relative positions of features in the SST and precipitation profiles between Codron (2012) and the present study, and attributing them to specific physical mechanisms, is challenging due to substantial evolution in the GCM (including its atmospheric model) between the two implementations. This is already evident when comparing the OHT-off configurations, which isolate the atmospheric component: the zonal-mean SST profiles in Fig.~XXX(a) (solid and dashed blue lines in this work and Codron (2012), respectively) differ markedly between the two studies.

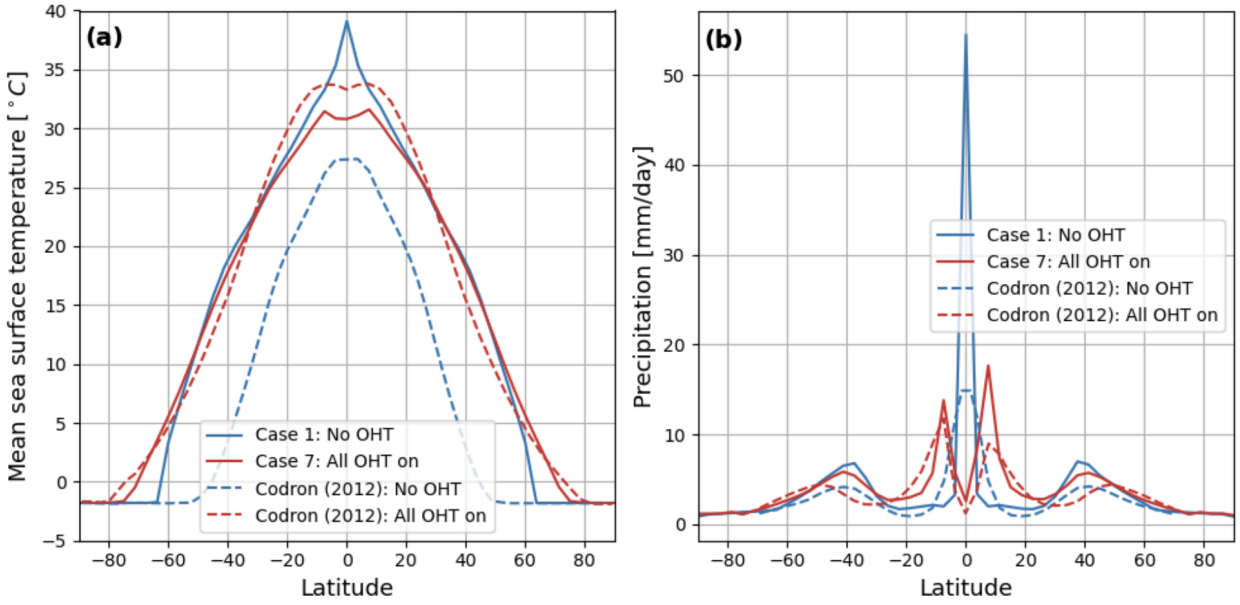

The large difference in equatorial temperatures in the OHT-off cases Fig.~XXX(a) directly affects the magnitude of the equatorial precipitation maxima (Fig.~XXX(b)). In Codron (2012), enabling OHT leads to a slight poleward shift of the storm tracks relative to the OHT-off case. A similar modest shift is observed in our study. However, it is unclear whether this reflects a physical response or a resolution-related artefact.

More generally, differences in profile shapes between Codron (2012) and this study likely reflect differences in atmospheric physics, particularly cloud / precipitation parameterisations, as well as the resolution (leading to stronger / weaker baroclinic eddies). These combined effects complicate direct one-to-one comparisons of individual climatic features."

Ln 345: "... (see Sect. 5.2 for more details).

For a more direct comparison, we also overlay the corresponding meridional OHT components from Codron (2012) in Fig.~XX. The total diffusive transport in the mid-latitudes (crossed grey lines in Codron, 2012; solid blue line in this work) is similar in both studies since the diffusion coefficients were tuned toward the same aquaplanet benchmark \citep{marshall2007mean}. *We* ***further*** *decompose the diffusive transport… … to the same amplitude as that seen in \cite{codron2012ekman}.* ***In contrast,***

Ekman transport in this work (solid green) exhibits larger amplitudes than in Codron (2012; grey circle-dotted line), in both the tropics and mid-latitudes, reaching values closer to the Eulerian ones in \citet{marshall2007mean}. This difference primarily arises due to GM transport in the present model. In addition to transporting heat downgradient, GM restratifies the two-layer ocean and strengthens Ekman transport. The poleward shifts of the mid-latitude Ekman trough and diffusive peak relative to Codron (2012) likely reflect differences in the atmospheric circulation between the two model versions, which influence surface wind stress and, in turn, OHT profiles. *With all components accounted for…"*

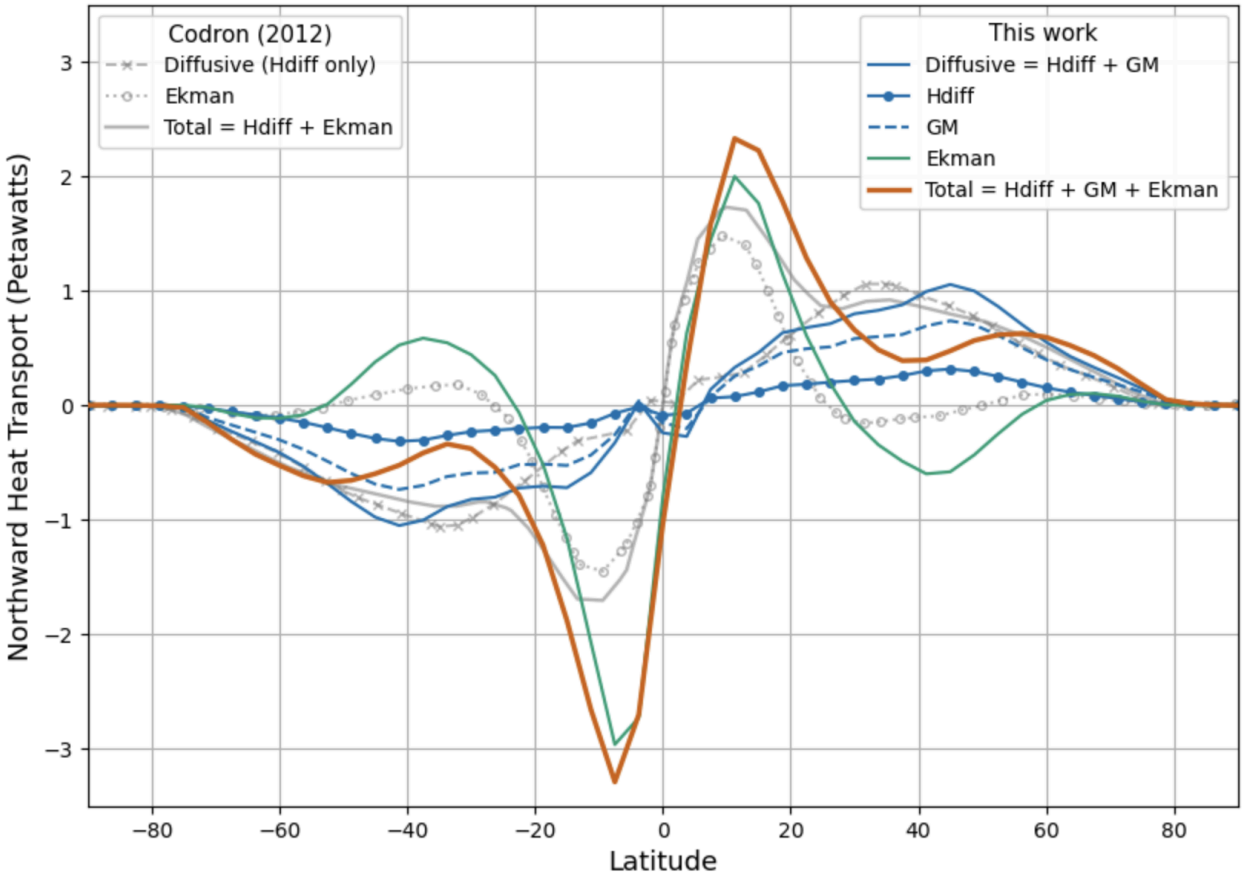

We thank the referee again for the constructive criticism. With the revisions detailed in this section and those to the specific comments below, we believe that our manuscript has been significantly strengthened.

Specific Comments

1. Line 1: Authors refer to this as a 'new' model, but also that it is building on a previous work. It is unclear to what extent this is an improvement on an existing model vs a novel model. This should be clarified / explained

We thank the referee for this helpful clarification. Indeed, this model builds on previous models and this should be better highlighted. We have modified the abstract as follows:

Ln 1: "We present ~~the new~~ ***an improved*** *dynamical slab ocean model implemented in a 3-D General Circulation Model (GCM) called the Generic Planetary Climate Model (Generic-PCM; formerly the LMD-Generic GCM).* ***Earlier two-layer slab ocean models featured wind-driven Ekman transport, horizontal diffusion and convective adjustment.*** *~~Our two-layer slab ocean model features emergent ocean heat transport (OHT) arising from wind-driven Ekman transport, horizontal diffusion, convective adjustment, and a newly implemented Gent–McWilliams (GM) parameterisation for mesoscale eddies. Sea ice evolution is spectrally dependent and varies with ice thickness.~~* ***Building upon this, our updated parallelised model introduces a Sverdrup balance scheme for Ekman transport, the first application of the Gent–McWilliams (GM) parameterisation of mesoscale eddies in a slab ocean model, and a spectrally dependent, thickness-dependent formulation of sea ice and snow albedo.****"*

For consistency, we also add text specifying this in the Introduction. Ln 123-127 had previously explicitly mentioned the new additions to the model compared to Codron (2012) and Charnay et al. (2013). A modified version of this has been moved to the Introduction instead and Ln 123-127 have been omitted to avoid repetition:

Ln 73-85: "This paper presents a ***follow-up of the model originally introduced by Codron (2012) and later adapted by Charnay et al. (2013). These earlier models included horizontal diffusion and convection, with Codron (2012) introducing, for the first time in a slab ocean model, wind-driven Ekman transport – the dominant driver of tropical meridional OHT in Earth observations (Levitus, 1987; Forget and Ferreira, 2019). Building upon this foundation, our work refines the two core processes historically handled by the dynamical slab ocean:***

(a) Sea ice evolution; with a spectral albedo representation, refined treatment of ice formation and melting, and the introduction of a finite heat capacity for snow (Section 2.2)

(b) Heat transport by ocean circulation; through optimised horizontal diffusion and Ekman transport, a Sverdrup balance scheme near the equator for more consistent tropical meridional transport (Section 2.3.1), and the implementation of mesoscale eddy mixing via the Gent-McWilliams parameterisation (Gent & McWilliams, 1990; Section 2.3.2), marking its first application within a slab ocean model.

The model is fully parallelised, enabling substantially faster integrations than earlier implementations and making it well suited for long simulations and ensemble studies, important in exoplanet and paleoclimate science. With these developments, our dynamical slab ocean model acts as a bridge between higher-level slab-oceans and fully coupled AOGCMs. *~~new "dynamical slab ocean model" that bridges the gap between higher-level slab-oceans and fully coupled AOGCMs. In our model, OHT is an emergent process that effectively couples the atmosphere and ocean. It includes~~*

~~*wind-driven Ekman transport - the dominant driver of tropical meridional OHT in Earth observations \citep{levitus1987meridional,forget2019global} -- along with horizontal diffusion and convection, following \citet{codron2012ekman} and \citet{charnay2013exploring}. Our model also introduces mesoscale eddy mixing in slab oceans through the Gent-McWilliams parameterisation \citep{gent1990isopycnal}, enabling horizontal and vertical temperature mixing. Additionally, sea ice evolution depends on ice thickness and the incoming spectra.*~~

~~*The model is designed to support large ensemble studies — a critical need in exoplanet and paleoclimate science, where observational constraints are sparse, motivating the exploration of a wide parameter space. Our goal is not to match the full complexity of AOGCMs, but to provide the modelling community a faster, physically grounded alternative - an improved compromise over traditional slab ocean models. This philosophy also aligns with the broader philosophy of intermediate-complexity GCMs like \textit{ExoPlaSim} \citep{paradise2022exoplasim}, which enable large-scale explorations of planetary climates while retaining core physical realism.*~~"

Ln 123-127: ~~*In this study, we improve the two key processes historically handled by the dynamical slab ocean: (a)*~~ ~~***Sea ice evolution***~~*, by improving the spectral albedo representation, refining sea ice formation, melting and freezing, and introducing a finite heat 125 capacity for snow (Sect. 2.2); and (b)*~~ ~~***Heat transport by ocean circulation***~~*, by optimising horizontal diffusion and Ekman transport, and implementing a new Gent–McWilliams (advection) parameterisation that captures both, the effect of mesoscale eddies and convection (Sect. 2.3). Furthermore, the model is now fully parallelised, enabling fast computation.*~~

2. Line 43-44: Salinity is mentioned here as important, but not included in the model. While the lack of salinity is returned to in the discussion, I think it would be good to discuss the omission of salinity somewhere in the introduction, perhaps here, or somewhere in lines 65-75 when the authors describe models of increasing complexity. I would suggest explaining here briefly why including salinity adds a disproportionately high computational cost for the improved accuracy.

We thank the referee for this relevant comment and have added a few lines to the modified text above of Comment #1 as follows:

Ln 73-85: "... ***marking its first application within a slab ocean model.***

Like in Codron (2012) and Charnay et al., (2013), our updated model does not include a prognostic salinity field or density-driven overturning circulation. While these processes are important in full AOGCMs (e.g., Cullum et al. 2016), they require solving additional tracer and density equations which substantially increases computational cost. Our model therefore focuses on wind-driven and eddy heat transport processes that capture the first-order meridional OHT while preserving computational efficiency.

***The model is fully parallelised…**”*

3. Line 406: Please refer specifically to what the reader should look at in figure 6c, and expand upon how this residual should be interpreted. I'm unsure from the text whether it is attributed to a physical phenomenon, or a model artefact

We have revised the text to explicitly indicate that the northward ITCZ shift in the OHT-off case is likely a model artefact. We also add context between Figure 6c and the text:

*Ln 405: “In our OHT-off simulation, the absence of OHT results in a near-equatorial ITCZ, slightly north-shifted ($\approx$ 3.5°N)~~,~~**. This displacement is** likely **a model artefact** ~~due to residual atmospheric processes (see Fig.~\ref{fig:OHT_Tslab1_Prec_Earth}c)~~. **Figure~\ref{fig:OHT_Tslab1_Prec_Earth}c shows the precipitation difference between the OHT-on and OHT-off simulations: a negative anomaly in the Northern Hemisphere and a positive one in the Southern Hemisphere indicates a southward migration of the ITCZ when OHT is enabled.** In the OHT-on case, ~~we find that~~ the ITCZ is positioned around 3.5°S. This ~~is due to~~ **shift arises from**: (a) the lack of density-driven MOC in our model, and (b), **enhanced Southern Hemisphere warming due to OHT-driven sea ice loss** ~~OHT causing sea ice loss in the Southern Hemisphere, resulting in excessive warming there~~. This Southern Hemisphere warming drives a northward atmospheric energy transport, which shifts the ITCZ ~~southward~~ to around 3.5°S, as shown in Fig.~\ref{fig:OHT_Tslab1_Prec_Earth}c. This behaviour is consistent …”*

4. line 524: space after bracket

For completeness, we omit the word “(exo-)” to generalise the statement.

Ln 523: “Furthermore, they highlight the importance of incorporating dynamic oceans in ~~(exo-)~~climate models, particularly when strong climate feedbacks…”

Modified abstract based on Referees 1 and 2

*“We present ~~the new~~ **an improved** dynamical slab ocean model implemented in a 3-D General Circulation Model (GCM) called the Generic Planetary Climate Model (Generic-PCM; formerly the LMD-Generic GCM). **Earlier two-layer slab ocean models featured wind-driven Ekman transport, horizontal diffusion and convective adjustment.** ~~Our two-layer slab ocean model features emergent ocean heat transport (OHT) arising from wind-driven Ekman transport, horizontal diffusion, convective adjustment, and a newly implemented Gent–McWilliams (GM) parameterisation for mesoscale eddies. Sea ice evolution is spectrally-dependent and varies with ice thickness.~~ **Building upon this, our updated parallelised model introduces a Sverdrup balance scheme for Ekman transport, the first application of the Gent–McWilliams (GM) parameterisation of mesoscale eddies in a slab ocean model, and a spectrally dependent, thickness-dependent formulation of sea ice and snow albedo.** We first validate the model in an idealised aquaplanet setting under various OHT configurations. We*

show that enabling OHT transforms not only surface features -- such as cooler tropical sea surface temperatures (SSTs) and reduced sea ice coverage -- but also atmospheric structures, notably producing a double-banded precipitation pattern across the equator driven by Ekman-induced upwelling. Our modelled meridional OHT profiles ~~are in~~ ***show first-order*** *agreement with fully coupled atmosphere-ocean GCMs, with Ekman transport dominating in the tropics* ***(fuelled by GM transport)*** *and* ***diffusion and*** *GM ~~advection~~* ***transport*** *~~and diffusion~~ peaking near the ice edge. When applied to modern Earth, the OHT-enabled configuration yields an annual global average surface temperature of 13°C, within 1°C of reanalysis estimates, and improves extrapolar SSTs and sea ice coverage relative to the OHT-disabled baseline. Seasonal SST and sea ice biases relative to observations are also significantly reduced to within 0.6°C and 3 million km², respectively. We obtain a planetary bond albedo of around 0.32, in close agreement with observations.* ***Together, the aquaplanet and modern Earth benchmarks demonstrate that the developments represent a clear improvement over earlier two-layer implementations.*** *~~We additionally find that GM-induced mixing mimics vertical convection, while the inclusion of OHT reduces hemispheric asymmetries and improves the overall GCM numerical stability.~~* ***We further show that GM-induced restratification reduces the need for explicit convective adjustment, while also strengthening Ekman transport. In addition to improving equatorial dynamics, the inclusion of the Sverdrup balance also reduces hemispheric asymmetries.*** *Notably,* ***due to model parallelisation,*** *these improvements are achieved at almost no additional computational cost compared to OHT-disabled simulations run over the same number of model years. This* ***enables long integrations and large ensemble studies, making the model particularly well suited for exoplanet and paleoclimate studies where broad parameter exploration is essential.*** *~~balance of computational efficiency and physical realism makes the model particularly well-suited for sensitivity studies and large parameter sweeps -- crucial in exoplanet and paleoclimate applications where observational constraints are limited.~~"*